

Qubit Reduction and Quantum Speedup for Wireless Channel Assignment Problem

Yuki Sano, Masaya Norimoto, *Graduate Student Member, IEEE*, and Naoki Ishikawa, *Senior Member, IEEE*.

Abstract—In this paper, we propose a novel method of formulating an NP-hard wireless channel assignment problem as a higher-order unconstrained binary optimization (HUBO), where the Grover adaptive search (GAS) is used to provide a quadratic speedup for solving the problem. The conventional method relies on a one-hot encoding of the channel indices, resulting in a quadratic formulation. By contrast, we conceive ascending and descending binary encodings of the channel indices, construct a specific quantum circuit, and derive the exact numbers of qubits and gates required by GAS. Our analysis clarifies that the proposed HUBO formulation significantly reduces the number of qubits and the query complexity compared with the conventional quadratic formulation. This advantage is achieved at the cost of an increased number of quantum gates, which we demonstrate can be reduced by our proposed descending binary encoding.

Index Terms—Quantum computing, channel assignment problem (CAP), combinatorial optimization, quadratic unconstrained binary optimization (QUBO), higher-order unconstrained binary optimization (HUBO).

I. INTRODUCTION

THE radio spectrum is a limited resource, whereas global mobile traffic is expected to increase 77-fold between 2020 and 2030 [1]. It is vital to support as many user terminals (UTs) as possible within the limited spectrum. To achieve efficient utilization of the spectrum, the problem of determining which channel access points (APs) should use is called the *channel assignment problem (CAP)*. It is known that CAP is equivalent to the generalized graph coloring problem [2], which is classified as NP-hard. CAP incurs a combinatorial explosion as the numbers of APs and UTs increase. Numerous greedy algorithms have been proposed [3] to obtain practical solutions within a limited amount of time, but none of them can guarantee that an optimal solution will be obtained.

In solving the NP-hard CAP, quantum annealing (QA) and the coherent Ising machine (CIM) have been demonstrated to be effective solutions. QA was used to solve the graph coloring problem [4]. It has been applied to the dynamic spectrum allocation problem and found to obtain a practical solution in a short time [5, 6]. CIM is another type of physical annealing system that outperforms QA for some specific problems [7]. Its application to the graph coloring problem is found in [8]. Hasegawa et al. formulated CAP as a quadratic unconstrained binary optimization (QUBO) problem and demonstrated that

CIM was capable of maximizing the channel capacity [9, 10]. It also succeeded in maximizing the total throughput of UTs in a dense Wi-Fi network [11]. In those conventional studies, both QA and CIM were demonstrated to be effective technologies for industrial applications. One remaining concern is that neither can guarantee their optimality, which is the same as other metaheuristics, including the greedy approach.

One promising approach that can guarantee global optimality is a quantum algorithm [12], *Grover adaptive search (GAS)* [13, 14], which relies on quantum superposition, entanglement, and amplitude amplification. Unlike QA and CIM, GAS supports higher-order unconstrained binary optimization (HUBO) problems in addition to QUBO problems. As with other Grover-type quantum algorithms [15–18], GAS provides quadratic speedups for solving QUBO and HUBO problems. That is, it achieves the query complexity of $O(\sqrt{2^n})$ with n binary variables, while the classic exhaustive search requires $O(2^n)$ function evaluations. Following the innovative GAS proposed by Gilliam et al. [13], an extension method that supports HUBO with real-valued coefficients was proposed in [19]. In addition, heuristic efforts and problem-specific attributes can be used to further reduce the constant overhead of GAS [20, 21]. The major challenge with quantum algorithms is the correction of quantum errors induced by noise [22]. Quantum algorithms, including GAS, require many physical qubits for quantum error correction [23] and share a common issue in terms of feasibility.

To reduce the number of required qubits and improve the feasibility, sophisticated formulations have been considered in the conventional studies: one-hot encoding and binary encoding. One-hot encoding indicates an index by a one-hot vector, such as $2 \rightarrow [0 \ 1 \ 0 \ 0]$ and $4 \rightarrow [0 \ 0 \ 0 \ 1]$, whereas binary encoding indicates an index by its binary representation, such as $2 \rightarrow [0 \ 1]$ and $4 \rightarrow [1 \ 1]$. In quantum computation, these encoding methods were first considered by Sawaya et al. [24] who aimed at improving the efficiency of quantum simulations.¹ Then, Fuchs et al. used the one-hot and binary encodings for the weighted Max-Cut problem and showed that the number of required qubits could be reduced by one logarithmic order [26]. Glos et al. used these encodings and formulated the traveling salesman problem as a HUBO problem [27]. Similarly, Tabi et al. used the binary encoding

Y. Sano, M. Norimoto, and N. Ishikawa are with the Faculty of Engineering, Yokohama National University, 240-8501 Kanagawa, Japan (e-mail: ishikawa-naoki-fr@ynu.ac.jp). This research was partially supported by the Japan Society for the Promotion of Science (JSPS) KAKENHI (Grant Number 22H01484) and the MITOU Program, Information-technology Promotion Agency, Japan.

¹The encoding method of Sawaya et al. was published on September 29, 2019 [24], which would be considered the first innovation in quantum computation. Note that in the context of the traveling salesman problem, Lidd's binary encoding of city indices was proposed in 1991 [25], but this contribution was limited to cross-over and mutation operations for genetic algorithms.

for the graph coloring problem and showed a reduction in the number of qubits [28]. Note that all the above conventional studies [26–28] considered the quantum approximate optimization algorithm (QAOA) for noisy intermediate-scale quantum computers rather than the GAS for fault-tolerant quantum computers.

Classically, the main approach to solving a HUBO problem is to transform it into a QUBO problem, and then use the semidefinite relaxation technique [29] to obtain a good but suboptimal solution in polynomial time. This transformation is termed *quadratization* [30, 31], and it involves an increase in the number of binary variables, resulting in an exponential increase in the search space size. By contrast, both QAOA and GAS can deal directly with HUBO problems owing to the interaction of multiple qubits, and do not impose the quadratic constraint required for the semidefinite relaxation.

Against this background, we propose a novel method of formulating CAP as a HUBO problem and analyze the numbers of qubits and gates required by GAS; this is a first attempt in the literature. The major contributions of this paper are summarized as follows.

- 1) We represent the channel indices as binary numbers and formulate the NP-hard CAP as a HUBO problem, whereas all the conventional studies [9–11] formulated CAP as a QUBO problem. Compared with the conventional QUBO formulation, the number of qubits required by GAS is significantly reduced by one logarithmic order, where a specific quantum circuit is constructed without any black-box quantum oracle.
- 2) For the conventional QUBO and the proposed HUBO formulations, we derive the exact numbers of required quantum gates and clarify corresponding asymptotic orders. Unlike the conventional studies [26–28], we conceive novel ascending and descending assignments for the binary encoding. The latter significantly reduces the number of quantum gates.
- 3) We confirm that the theoretical speedup by GAS is also effective for CAP. Here, the proposed HUBO formulation significantly reduces the query complexity in the classical domain compared with the conventional QUBO owing to the reduced search space caused by the reduced number of qubits.

The remainder of this paper is organized as follows. In Section II, we introduce the conventional GAS that supports real-valued coefficients. Section III is a review of the conventional QUBO formulation for CAP, while in Section IV, we propose our HUBO formulation. For both formulations, algebraic and numerical evaluations are given in Section V. Finally, in Section VI, we conclude this paper. Italicized symbols represent scalar values, and bold symbols represent vectors and matrices. Table I summarizes the important mathematical symbols used in this paper.

II. GROVER ADAPTIVE SEARCH [13, 19]

In this section, we introduce the innovative GAS algorithm proposed by Gilliam et al. [13] and its modification to support real-valued coefficients [19]. GAS is a quantum algorithm

TABLE I
LIST OF IMPORTANT MATHEMATICAL SYMBOLS

\mathbb{B}		Binary numbers
\mathbb{R}		Real numbers
\mathbb{C}		Complex numbers
\mathbb{Z}		Integers
j	$\in \mathbb{C}$	Imaginary number
N_{AP}	$\in \mathbb{Z}$	Number of APs
N_{CH}	$\in \mathbb{Z}$	Number of channels
N_{B}	$\in \mathbb{Z}$	Number of bits required to represent N_{CH} channel indices, i.e., $N_{\text{B}} = \lceil \log_2 N_{\text{CH}} \rceil$
B_{w}	$\in \mathbb{R}$	Bandwidth
P	$\in \mathbb{R}$	Transmit power
x	$\in \mathbb{B}$	Binary variable
$E(x)$	$\in \mathbb{Z}$	Conv. objective function for QUBO
$E'(x)$	$\in \mathbb{Z}$	Prop. objective function for HUBO
G	$\in \mathbb{Z}$	Number of gates required by conv. QUBO
G'	$\in \mathbb{Z}$	Number of gates required by prop. HUBO
i, k	$\in \mathbb{Z}$	Index of APs or GAS iterations
c, l	$\in \mathbb{Z}$	Index of channels
d_{iu}	$\in \mathbb{R}$	Physical distance between i th AP and u th UT
α	$\in \mathbb{R}$	Attenuation coefficient
n	$\in \mathbb{Z}$	Number of QUBO variables in $E(x)$
m	$\in \mathbb{Z}$	Number of qubits required to encode $E(x)$
n'	$\in \mathbb{Z}$	Number of HUBO variables in $E'(x)$
m'	$\in \mathbb{Z}$	Number of qubits required to encode $E'(x)$
y_i	$\in \mathbb{Z}$	Threshold that is adaptively updated by GAS
L_i	$\in \mathbb{Z}$	Number of Grover operators

that solves QUBO and HUBO problems owing to its efficient construction method for the corresponding quantum circuit. It requires $n + m$ qubits [13]², where n is the number of binary variables and m is the number of qubits to encode the objective function value using the two's complement representation. Therefore, m is the smallest integer that satisfies the following two inequalities:

$$-2^{m-1} \leq a < 2^{m-1} \quad (1)$$

and

$$-2^{m-1} \leq \min[E(x)] \leq \max[E(x)] < 2^{m-1}. \quad (2)$$

Here, a is an arbitrary coefficient included in the objective function $E(x)$, which is a quadratic or higher-order polynomial function of n binary variables (x_1, \dots, x_n) . GAS minimizes the objective function $E(x)$ by two steps: (1) create an equal superposition of 2^n quantum states and (2) amplify the states of interest where the values of the objective function become smaller than the current minimum. If the objective function $E(x)$ contains real-valued coefficients, multiple states may be amplified depending on the value, resulting in a superposition of approximated integers [13]. That is, there is a slight probability that inappropriate states will be observed, in which case, GAS may not work. This inappropriate behavior can be avoided if the algorithm calibrates the objective function value to the correct one in the classical domain. At the sacrifice of additional query complexity in the classical domain, the modified GAS [19] supports real-valued coefficients of QUBO and HUBO functions.

In [13], Gilliam et al. proposed an efficient method to construct a quantum circuit corresponding to a binary polynomial function $E(x)$. We introduce this construction method using

²In practice, some ancillae are required, which is detailed in Section V.

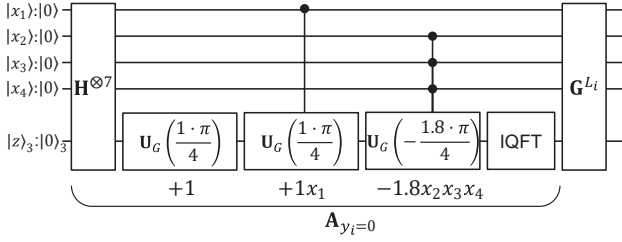


Fig. 1. Quantum circuit corresponding to $E(x) = 1 + x_1 - 1.8x_2x_3x_4$ and $y_i = 0$.

the example quantum circuit shown in Fig. 1, corresponding to $E(x) = 1 + x_1 - 1.8x_2x_3x_4$. Specifically, at an iteration index i , a state preparation operator \mathbf{A}_{y_i} calculates values $E(x) - y_i$ corresponding to 2^n states, where y_i is the current minimum. Here, the two's complement is used to represent negative values. The operator \mathbf{A}_{y_i} is composed of the inverse quantum Fourier transform (IQFT), the Hadamard gates

$$\mathbf{H} = \frac{1}{\sqrt{2}} \begin{bmatrix} +1 & +1 \\ +1 & -1 \end{bmatrix}, \quad (3)$$

$$\mathbf{H}^{\otimes n} = \underbrace{\mathbf{H} \otimes \cdots \otimes \mathbf{H}}_{n \text{ gates}} \quad (4)$$

that creates an equal superposition, the phase gate

$$\mathbf{R}(\theta) = \begin{bmatrix} 1 & 0 \\ 0 & e^{j\theta} \end{bmatrix}, \quad (5)$$

and the unitary operator [13]

$$\mathbf{U}_G(\theta) = \mathbf{R}(2^{m-1}\theta) \otimes \mathbf{R}(2^{m-2}\theta) \otimes \cdots \otimes \mathbf{R}(2^0\theta), \quad (6)$$

where we have $\theta = 2\pi a/2^m$. The unitary operator $\mathbf{U}_G(\theta)$ corresponds to a coefficient a in the objective function, and it is controlled by a set of qubits corresponding to binary variables. For example, as shown in Fig. 1, the term $+1$ corresponds to the gate $\mathbf{U}_G(+1 \cdot \pi/4)$ and the term $-1.8x_2x_3x_4$ corresponds to the gate $\mathbf{U}_G(-1.8 \cdot \pi/4)$ controlled by $(|x_2\rangle, |x_3\rangle, |x_4\rangle)$. The states of interest, in which the values $E(x) - y_i$ become negative, can be identified by focusing on the beginning of m qubits since we use the two's complement. Then, the oracle operator \mathbf{O} has a single Z gate

$$\mathbf{Z} = \begin{bmatrix} 1 & 0 \\ 0 & -1 \end{bmatrix} \quad (7)$$

to invert the phase of the negative states, i.e.,

$$\mathbf{O} = \underbrace{\mathbf{I}_2 \otimes \cdots \otimes \mathbf{I}_2}_n \otimes \mathbf{Z} \otimes \underbrace{\mathbf{I}_2 \otimes \cdots \otimes \mathbf{I}_2}_{m-1} \quad (8)$$

The Grover operator $\mathbf{G} = \mathbf{A}_{y_i} \mathbf{D} \mathbf{A}_{y_i}^H \mathbf{O}$ amplifies only such states and is composed of \mathbf{A}_{y_i} , \mathbf{O} , and the Grover diffusion operator \mathbf{D} [13].

In GAS, to amplify the states of interest, the Grover operator \mathbf{G} is applied L_i times, which is a uniform random value. After that, the quantum states are measured, and a solution (x_1, \dots, x_n) is obtained. To calibrate the mismatch induced by the real-valued coefficients, the objective function value $y = E(x)$ is evaluated in the classical domain, and

Algorithm 1 GAS supporting real-valued coefficients [13, 19].

Input: $E(x) : \mathbb{B}^n \rightarrow \mathbb{R}, \lambda = 8/7$

Output: x_1, \dots, x_n

- 1: Uniformly sample x_1, \dots, x_n and set $y_0 = E(x)$.
- 2: Set $k = 1$ and $i = 0$.
- 3: **repeat**
- 4: Let L_i be a random number from 0 to $\lceil k-1 \rceil$.
- 5: Evaluate $\mathbf{G}^{L_i} \mathbf{A}_{y_i} |0\rangle_{n+m}$ and obtain x'_1, \dots, x'_n .
- 6: Evaluate $y = E(x')$ in the classical domain. {This is an additional step to support real coefficients}
- 7: **if** $y < y_i$ **then**
- 8: Update the solution $x_1 = x'_1, \dots, x_n = x'_n$.
- 9: Set $y_{i+1} = y$ and $k = 1$.
- 10: **else**
- 11: Set $y_{i+1} = y_i$ and $k = \min\{\lambda k, \sqrt{2^m}\}$.
- 12: **end if**
- 13: $i = i + 1$.
- 14: **until** a termination condition is met.

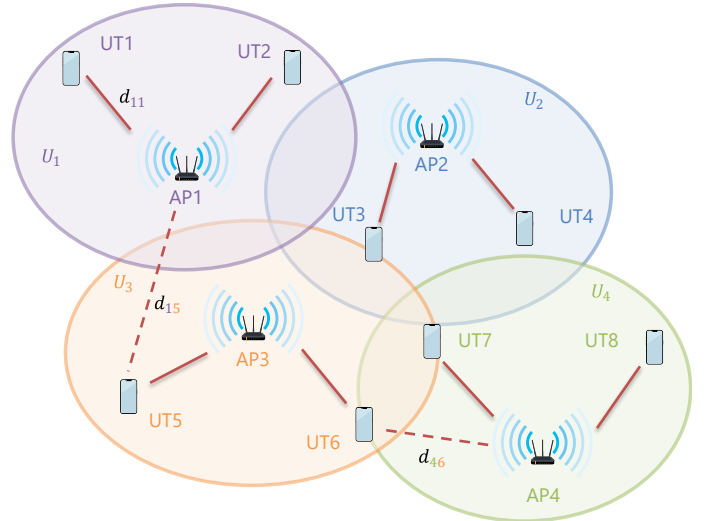


Fig. 2. System model of CAP, where the number of APs is $N_{AP} = 4$ and the number of channels is $N_{CH} = 3$.

is compared with the current minimum value y_i . If the value is smaller than y_i , GAS updates the solution and the current minimum, and sets $k = 1$. Otherwise, GAS sets $k = \min\{\lambda k, \sqrt{2^m}\}$ using a scalar $\lambda = 8/7$ [16, 32]. The termination condition could be based on the sum of the number of Grover operators, the number of classical iterations, or the number of iterations in which the objective value does not improve. The above algorithm is summarized in Algorithm 1.

III. CONVENTIONAL QUBO FORMULATION WITH ONE-HOT ENCODING [9–11]

In this section, we review a conventional QUBO formulation for CAP, which relies on the one-hot encoding of channel indices. Let the number of APs be N_{AP} and the number of channels be N_{CH} , and we assume that the condition $N_{CH} < N_{AP}$ holds.³ Fig. 2 shows an example system setup of CAP,

³When $N_{CH} \geq N_{AP}$, the optimal solution for CAP is obvious.

where we consider $N_{\text{AP}} = 4$ APs, $N_{\text{CH}} = 3$ channels, and eight UTs. Here, U_i denotes a set of UTs associated with the i th AP for $1 \leq i \leq N_{\text{AP}}$. In Fig. 2, two UTs are associated with each AP. The scalar constant d_{iu} denotes the physical distance between the i th AP and u th UT. The search space size is calculated as

$$C_{\text{CAP}} = N_{\text{CH}}^{N_{\text{AP}}}, \quad (9)$$

which is not clarified in [9–11].

In the conventional studies [9–11], the goal is to maximize the total capacity of the network

$$\sum_{i=1}^{N_{\text{AP}}} B_w \log_2 \left(1 + \frac{S_i}{I_i + N_i} \right), \quad (10)$$

where S_i is the power of the received signal of interest at i th AP, I_i is the interference power from other APs, N_i is the noise power, and B_w is the bandwidth. In the following, we consider maximization of the total capacity. Although some studies [9, 10] considered maximizing the sum of signal-to-interference-plus-noise ratios (SINRs), the essential formulation approach below is identical with the conventional studies [9–11]. Maximizing (10) is equivalent to minimizing

$$-\sum_{i=1}^{N_{\text{AP}}} \log_2 \left(1 + \frac{S_i}{I_i} \right), \quad (11)$$

which is considered as an objective function. Then, we prepare $N_{\text{AP}}N_{\text{CH}}$ binary variables defined by [9, 10]

$$x_{ic} = \begin{cases} 1 & \text{the } i\text{th AP uses the } c\text{th channel} \\ 0 & \text{otherwise} \end{cases} \quad (12)$$

for $1 \leq i \leq N_{\text{AP}}$ and $1 \leq c \leq N_{\text{CH}}$. Since the i th AP uses a single channel, $[x_{i1} \cdots x_{iN_{\text{CH}}}] \in \mathbb{B}^{N_{\text{CH}}}$ becomes a one-hot vector; this is also known as one-hot encoding.

Assuming a simplified path-loss channel model, the received signal power of interest at i th AP is represented by

$$\sum_{u \in U_i} P d_{iu}^{-\alpha} \quad (13)$$

where P denotes the transmit power, U_i denotes a set of UTs associated with the i th AP, d_{iu} denotes the distance between the i th AP and u th UT, and α denotes an attenuation coefficient. Similarly, the total interference at i th AP from other APs is represented by

$$\sum_{c=1}^{N_{\text{CH}}} \sum_{k=1}^{N_{\text{AP}}} \sum_{l=1}^{N_{\text{CH}}} \left(\sum_{v \in U_k} P d_{iv}^{-\alpha} \right) \delta_{cl} (1 - \delta_{ik}) x_{ic} x_{kl}, \quad (14)$$

where δ_{cl} denotes the Kronecker delta defined by

$$\delta_{cl} = \begin{cases} 1 & \text{if } c = l \\ 0 & \text{otherwise.} \end{cases} \quad (15)$$

That is, the term $\delta_{cl}(1 - \delta_{ik})x_{ic}x_{kl}$ becomes 1 if a pair (i, k) of different APs use the same channel $c = l$, and 0 otherwise.

From (13) and (14), minimizing (11) is equivalent to minimizing

$$E_1(x) = \sum_{i=1}^{N_{\text{AP}}-1} \sum_{c=1}^{N_{\text{CH}}} \sum_{k=i+1}^{N_{\text{AP}}} \sum_{l=1}^{N_{\text{CH}}} D_{ik} \delta_{cl} (1 - \delta_{ik}) x_{ic} x_{kl}, \quad (16)$$

where we have

$$D_{ik} = C_{ik} - C_{\min} + \epsilon, \quad (17)$$

and

$$C_{ik} = -\log_2 \left(1 + \frac{\sum_{u \in U_i} d_{iu}^{-\alpha}}{\sum_{v \in U_k} d_{iv}^{-\alpha}} \right) - \log_2 \left(1 + \frac{\sum_{u \in U_k} d_{ku}^{-\alpha}}{\sum_{v \in U_i} d_{kv}^{-\alpha}} \right). \quad (18)$$

Here, ϵ is a small constant such as $\epsilon = 0.01$, and C_{\min} is the minimum of C_{ik} for $1 \leq i < k \leq N_{\text{AP}}$. Both parameters ϵ and C_{\min} lead to $D_{ik} > 0$. In addition, each AP uses a single channel. This constraint can be given by [9–11]

$$E_2(x) = \sum_{i=1}^{N_{\text{AP}}} \left(\sum_{c=1}^{N_{\text{CH}}} x_{ic} - 1 \right)^2. \quad (19)$$

Overall, from (16) and (19), CAP is formulated as [9–11]

$$\begin{aligned} \min_x \quad & E(x) = E_1(x) + w E_2(x) \\ \text{s.t.} \quad & x_{ic} \in \mathbb{B} \end{aligned} \quad (20)$$

for $1 \leq i \leq N_{\text{AP}}$ and $1 \leq c \leq N_{\text{CH}}$. Here, w is a penalty parameter for satisfying the constraint of $E_2(x)$. The objective function $E(x)$ is a quadratic function using the one-hot encoding of channel indices. A specific example of QUBO formulation is given in Appendix A.

IV. PROPOSED HUBO FORMULATION WITH BINARY ENCODING

As reviewed in Section III, the conventional QUBO formulation relies on the one-hot encoding. In this section, a novel HUBO formulation using the binary encoding is proposed, which is solved by the GAS introduced in Section II.

As with the original QUBO formulation [9–11], the goal is to maximize the total capacity (10) of the network. The original formulation requires $N_{\text{AP}}N_{\text{CH}}$ binary variables x_{ic} to represent the state where the i th AP uses the c th channel. That is, the search space size of the QUBO formulation is calculated as

$$C_{\text{QUBO}} = 2^{N_{\text{AP}}N_{\text{CH}}}, \quad (21)$$

which is larger than the original search space $C_{\text{CAP}} = N_{\text{CH}}^{N_{\text{AP}}}$ of (9). According to (9), it can be expected that the minimum number of required binary variables is calculated as

$$\log_2 C_{\text{CAP}} = N_{\text{AP}} \log_2 N_{\text{CH}}. \quad (22)$$

In the following, we conceive an optimal formulation that can achieve the minimum number (22), resulting in the minimum size of search space. Since $\log_2 N_{\text{CH}}$ is included in (22), it can be expected that the channel index should be represented by a binary number. The number of bits N_{B} required to represent N_{CH} channel indices is

$$N_{\text{B}} = \lceil \log_2 N_{\text{CH}} \rceil \quad (23)$$

because we have $2^{N_{\text{B}}-1} < N_{\text{CH}} \leq 2^{N_{\text{B}}}$. Since N_{CH} is not limited to a power of two, it may allocate up to one bit more than the original search space, which is inefficient.

TABLE II
PROPOSED ASCENDING AND DESCENDING BINARY ENCODINGS.

Index	Binary encoding (asc.)	Binary encoding (desc.)
c	$[b_{c1} \ b_{c2}], \ \delta'_{ic}(x)$	$[b_{c1} \ b_{c2}], \ \delta'_{ic}(x)$
1	$[0 \ 0], \ (1 - x_{i1})(1 - x_{i2})$	$[1 \ 1], \ x_{i1}x_{i2}$
2	$[0 \ 1], \ (1 - x_{i1})x_{i2}$	$[1 \ 0], \ x_{i1}(1 - x_{i2})$
3	$[1 \ 0], \ x_{i1}(1 - x_{i2})$	$[0 \ 1], \ (1 - x_{i1})x_{i2}$

Here, we propose an encoding method of exploiting the unallocated bit and reducing the number of terms included in a new objective function. Specifically, we assign N_B -bit sequences, starting from all zeros, to the ascending channel indices $c = 1, 2, \dots, N_{CH}$, which is referred to as *ascending binary encoding*. In this encoding method, given the channel index c , an N_B -bit sequence is defined by

$$[b_{c1} \ b_{c2} \ \dots \ b_{cN_B}] = [c - 1]_2, \quad (24)$$

where $[\cdot]_2$ denotes the decimal to binary conversion. By contrast, in another method, we assign the bit sequences to the descending channel indices $c = N_{CH}, N_{CH} - 1, \dots, 1$, which is referred to as *descending binary encoding*. In this descending binary encoding, an N_B -bit sequence is defined by

$$[b_{c1} \ b_{c2} \ \dots \ b_{cN_B}] = [N_{CH} - c + 1]_2. \quad (25)$$

For both encoding methods, the state where the i th AP uses the c th channel is represented by

$$\delta'_{ic}(x) = \prod_{r=1}^{N_B} (1 - b_{cr} + (2b_{cr} - 1)x_{ir}), \quad (26)$$

where we have $N_{AP}N_B$ binary variables x_{ir} for $1 \leq i \leq N_{AP}$ and $1 \leq r \leq N_B$. Note that $\delta'_{ic}(x)$ is a function of order N_B .

In the proposed encoding methods, the interference between APs is represented by

$$E'_1(x) = \sum_{i=1}^{N_{AP}-1} \sum_{k=i+1}^{N_{AP}} D_{ik} \sum_{c=1}^{N_{CH}} \delta'_{ic}(x) \delta'_{kc}(x), \quad (27)$$

which should be minimized. Additionally, when $N_{CH} < 2^{N_B}$, we add

$$E'_2(x) = \sum_{i=1}^{N_{AP}} \sum_{c=N_{CH}+1}^{2^{N_B}} \delta'_{ic}(x) \quad (28)$$

due to the constraint that each AP does not use nonexistent channels. Overall, from (27) and (28), the proposed HUBO formulation is given by

$$\begin{aligned} \min_x \quad & E'(x) = E'_1(x) + w' E'_2(x) \\ \text{s.t.} \quad & x_{ir} \in \mathbb{B}, \end{aligned} \quad (29)$$

where w' is a penalty parameter for satisfying the constraint of $E'_2(x)$. The proposed objective function contains terms of the order $2N_B$ at most. That is, it is a unique HUBO formulation that can be solved by GAS.

Let us check a specific example in which $N_{AP} = 4$, $N_{CH} = 3$, and $N_B = \lceil \log_2 3 \rceil = 2$. Table II provides the mapping between the channel indices $c = 1, 2, 3$, the

binary sequence $[b_{c1} \ b_{c2}]$, and the function $\delta'_{ic}(x)$, where both ascending and descending binary encodings are considered. The number of terms in $(1 - x_{i1})(1 - x_{i2})$ is four, while it is reduced to one in $x_{i1}x_{i2}$. The corresponding HUBO formulations are given in (58) and (59) of Appendix B. Fig. 3 shows a quantum circuit corresponding to (59), where we have $n' = 8$ and $m' = 4$ qubits. As shown in Fig. 3, the Hadamard gate $\mathbf{H}^{\otimes 12}$ at the beginning creates an equal superposition state. The unitary operators such as $\mathbf{U}_G(4.000 \cdot \pi/8)$ and $\mathbf{U}_G(5.505 \cdot \pi/8)$ correspond to the coefficients 4.000 and 5.505. Some unitary operators are controlled depending on the associated binary variables.

V. ALGEBRAIC AND NUMERICAL ANALYSIS

In this section, we analyze both conventional and proposed formulations in terms of (1) the number of binary variables, (2) the number of qubits, (3) the number of gates, and (4) query complexity. The numbers of qubits and gates are derived in an algebraic manner and the corresponding asymptotic orders are given using the big-Omicron notation $O(\cdot)$ of [33].

A. Number of Binary Variables

The number of binary variables determines the size of the search space and the rate of convergence to the optimal solution. In the conventional QUBO formulation (20), the number of binary variables is

$$n = N_{AP}N_{CH}. \quad (30)$$

By contrast, in the proposed HUBO formulation (29), the number of binary variables is

$$n' = N_{AP}N_B = N_{AP} \lceil \log_2 N_{CH} \rceil, \quad (31)$$

which is valid for both ascending and descending binary encodings. Since the search space size of CAP is $(N_{CH})^{N_{AP}}$, the proposed formulation becomes optimal if N_{CH} is a power of two.

In the conventional studies, the HUBO problems have been solved by transforming the objective function to a quadratic form [31]; this is termed *quadratzation*. A representative quadratzation approach [30] replaces a product of two binary variables with a single auxiliary binary variable and adds a constraint term to the objective function. For example, if we have the HUBO function $f(x) = x_1x_2x_3$, the product x_1x_2 is replaced with a new auxiliary variable y , and the following term,

$$x_1x_2 - 2x_1y - 2x_2y + 3y, \quad (32)$$

is added to the original objective function so that the constraint $x_1x_2 = y$ holds. Here, it is crucial to multiply (32) by a scaling factor, which requires additional parameter tuning. If the objective function is of order four or higher, the above replacement is repeated in a recursive manner. Following the quadratzation approach [30], the proposed HUBO function can be transformed into a quadratic form that has

$$n'' = N_{AP}N_B + N_{AP} \sum_{r=2}^{N_B} \binom{N_B}{r} = N_{AP}(2^{N_B} - 1) \quad (33)$$

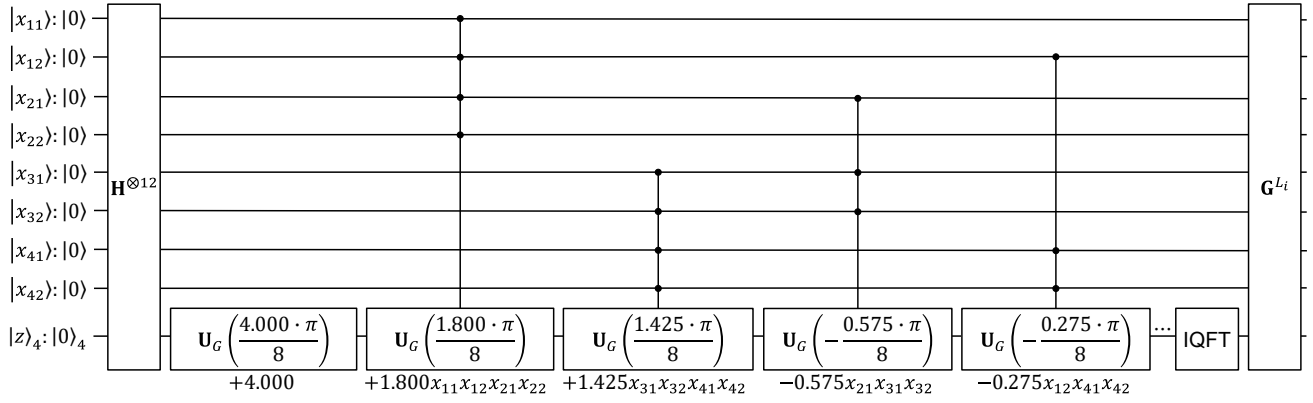


Fig. 3. Quantum circuit corresponding to objective function (59).

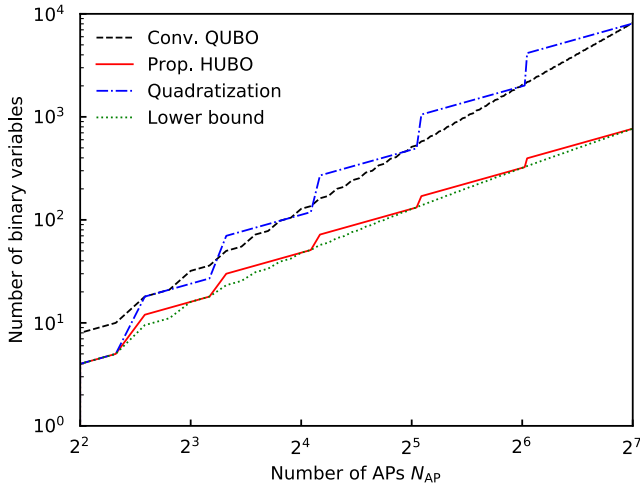


Fig. 4. Actual numbers of binary variables.

binary variables.

From (30) and (31), $n' < n$ holds for $N_{\text{CH}} \geq 2$, and from (31) and (33), $n' < n''$ holds for $N_{\text{CH}} \geq 3$. Hence, the proposed formulation achieves the minimum among the considered formulations. Additionally, from (30) and (33), $n \leq n''$ holds in most cases. However, surprisingly, if N_{CH} is a power of two, $n > n'' = n - N_{\text{AP}}$ holds.

In Fig. 4, we plot the actual numbers of binary variables required by the conventional QUBO, the proposed HUBO, and the QUBO transformed from HUBO (quadratzation), where we fixed $N_{\text{CH}} = \lfloor N_{\text{AP}}/2 \rfloor$ for illustration. As shown in Fig. 4, the number of binary variables for the proposed HUBO was close to the lower bound, $\log_2 C_{\text{CAP}}$, and was much smaller than for the other formulations. Additionally, when $(N_{\text{AP}}, N_{\text{CH}}) = (128, 64)$, the QUBO formulation transformed from HUBO required 8064 binary variables, which was less than the 8192 of the conventional QUBO. Here, the number of binary variables was reduced by $8192 - 8064 = 128 = N_{\text{AP}}$, indicating that the search space is reduced by $1/2^{128}$.

B. Number of Qubits

As introduced in Section II, GAS [13, 19] requires $n + m$ qubits, where n denotes the number of binary variables and m denotes the number of qubits used for encoding the value of the objective function. Since m must satisfy inequalities (1) and (2), we investigate the minimum and maximum objective functions $E(x)$ and $E'(x)$, where the ascending binary encoding is considered for the proposed HUBO.⁴

According to (20), in the original QUBO formulation, the minimum of the objective function is

$$0 \leq \min(E(x)) < D_{\text{sum}}, \quad (34)$$

and the maximum is

$$\max(E(x)) = N_{\text{CH}} D_{\text{sum}} + w N_{\text{AP}} (N_{\text{CH}} - 1)^2, \quad (35)$$

where we have

$$D_{\text{sum}} = \sum_{i=1}^{N_{\text{AP}}-1} \sum_{k=i+1}^{N_{\text{AP}}} D_{ik}. \quad (36)$$

Then, the number of qubits required to encode $E(x)$ can be calculated as

$$m = \lceil \log_2(\max(E(x))) \rceil + 1, \quad (37)$$

and the total number of required qubits is

$$\begin{aligned} n + m &= N_{\text{AP}} N_{\text{CH}} + \lceil \log_2(N_{\text{CH}} D_{\text{sum}} + w N_{\text{AP}} (N_{\text{CH}} - 1)^2) \rceil + 1 \\ &= O(N_{\text{AP}} N_{\text{CH}}), \end{aligned} \quad (38)$$

which indicates that the number of binary variables has the dominant effect.

In the proposed HUBO formulation, from (58) and (59), the minimum of the objective function is

$$0 \leq \min(E'_a(x)) = \min(E'_d(x)) < D_{\text{sum}}, \quad (39)$$

and the maximum is

$$\max(E'_a(x)) = \max(E'_d(x)) = \sum_{i=1}^{N_{\text{AP}}-1} \sum_{k=i+1}^{N_{\text{AP}}} D_{ik} = D_{\text{sum}}. \quad (40)$$

⁴The proposed ascending and descending encodings lead to the same minimum and maximum values.

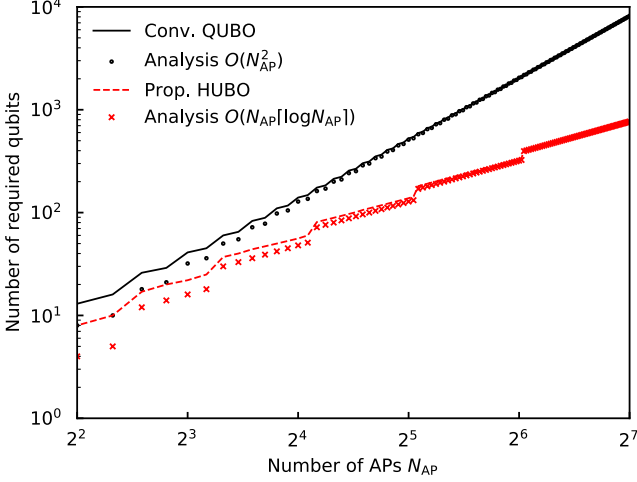


Fig. 5. Numbers of required qubits, with lines indicating actual values and markers indicating theoretical values.

Then, the number of qubits required to encode $E'_a(x)$ or $E'_d(x)$ can be calculated as

$$m' = \lceil \log_2(\max(E'_a(x))) \rceil + 1, \quad (41)$$

and the total number of required qubits is

$$\begin{aligned} n' + m' &= N_{\text{AP}} \lceil \log_2 N_{\text{CH}} \rceil + \lceil \log_2 D_{\text{sum}} \rceil + 1 \\ &= O(N_{\text{AP}} \lceil \log N_{\text{CH}} \rceil). \end{aligned} \quad (42)$$

Since $N_{\text{CH}} > \lceil \log_2 N_{\text{CH}} \rceil$ and $w > 0$ hold, the number of required qubits for the proposed HUBO is less than that for the conventional QUBO, i.e., $n' < n$ and $m' < m$.

To simplify the comparison, we fix both the distance D_{ik} and the penalty factor w to 1, and fix the number of channels to $N_{\text{CH}} = \lfloor N_{\text{AP}}/2 \rfloor$. In this simplified case, D_{sum} becomes $N_{\text{AP}}(N_{\text{AP}} - 1)/2$. Then, the conventional formulation requires $n + m = O(N_{\text{AP}}^2)$ qubits, while the proposed formulation requires $n' + m' = O(N_{\text{AP}} \lceil \log N_{\text{AP}} \rceil)$ qubits. In Fig. 5, we plot the derived order as well as the actual number of qubits required by constructed circuits. As shown in Fig. 5, both analytical and numerical values basically corresponded, demonstrating the accuracy of our analysis. The proposed formulation succeeded in reducing the number of required qubits without exception. Although the effect of the non-negligible terms is large when N_{AP} is small, the quadratic speedup by GAS is particularly dominant when the problem size is large.

C. Number of Gates

The number of quantum gates is an important evaluation metric because it determines the feasibility of quantum circuits and quantum algorithms. As in the conventional studies [13, 19], we construct a specific quantum circuit using GAS and count the number of quantum gates. In the quantum circuit of GAS, the most complex part is the gates corresponding to \mathbf{A}_{y_i} . In the following, we analyze the number of gates used in \mathbf{A}_{y_i} .

In the conventional QUBO formulation, from (38), the number of H gates is

$$G_{\text{H}} = n + m = O(N_{\text{AP}} N_{\text{CH}}). \quad (43)$$

The numbers of R and controlled R (CR) gates can be calculated using (37). The number of terms of the first order corresponds to the number of 1-CR gates, which is calculated as

$$\begin{aligned} G_{1\text{-CR}} &= N_{\text{AP}} N_{\text{CH}} \beta \\ &= O(N_{\text{AP}} N_{\text{CH}} \log(N_{\text{AP}}^2 N_{\text{CH}} + N_{\text{AP}} N_{\text{CH}}^2)), \end{aligned} \quad (44)$$

where we have

$$\begin{aligned} \beta &= \left\lceil \log_2 \left(N_{\text{CH}} \binom{N_{\text{AP}}}{2} + N_{\text{AP}} (N_{\text{CH}} - 1)^2 \right) \right\rceil + 1 \\ &= \log_2 \left(N_{\text{CH}} \binom{N_{\text{AP}}}{2} + N_{\text{AP}} (N_{\text{CH}} - 1)^2 \right) + O(1). \end{aligned} \quad (45)$$

Similarly, we count the number of quadratic terms in the objective function. The corresponding number of 2-CR gates is calculated as

$$\begin{aligned} G_{2\text{-CR}} &= \left(N_{\text{CH}} \binom{N_{\text{AP}}}{2} + N_{\text{AP}} \binom{N_{\text{CH}}}{2} \right) \cdot \beta \\ &= \frac{N_{\text{AP}} N_{\text{CH}} (N_{\text{AP}} + N_{\text{CH}} - 2)}{2} \cdot \beta \\ &= O(N_{\text{AP}} N_{\text{CH}} (N_{\text{AP}} + N_{\text{CH}}) \log(N_{\text{AP}}^2 N_{\text{CH}} + N_{\text{AP}} N_{\text{CH}}^2)). \end{aligned} \quad (46)$$

In the proposed HUBO formulation, from (42), the number of H gates is

$$G'_{\text{H}} = n' + m' = O(N_{\text{AP}} \log N_{\text{CH}}). \quad (47)$$

The numbers of R and CR gates are calculated using (41). Specifically, the number of 1-CR gates is calculated as

$$\begin{aligned} G'_{1\text{-CR}} &= N_{\text{AP}} N_{\text{B}} \cdot \beta' = N_{\text{AP}} \lceil \log_2 N_{\text{CH}} \rceil \cdot \beta' \\ &= O(N_{\text{AP}} \log N_{\text{AP}} \log N_{\text{CH}}) \end{aligned} \quad (48)$$

where we have

$$\beta' = \left\lceil \log_2 \binom{N_{\text{AP}}}{2} \right\rceil + 1 = O(\log N_{\text{AP}}). \quad (49)$$

Similarly, the number of 2-CR gates is

$$\begin{aligned} G'_{2\text{-CR}} &= \binom{N_{\text{AP}} N_{\text{B}}}{2} \cdot \beta' = \frac{N_{\text{AP}} N_{\text{B}} (N_{\text{AP}} N_{\text{B}} - 1)}{2} \cdot \beta' \\ &= O(N_{\text{AP}}^2 \log N_{\text{AP}} (\log N_{\text{CH}})^2). \end{aligned} \quad (50)$$

Additionally, the number of k -CR gates is

$$\begin{aligned} G'_{k\text{-CR}} &= \left\{ \binom{N_{\text{AP}}}{2} \binom{2N_{\text{B}}}{k} - N_{\text{AP}} (N_{\text{AP}} - 2) \binom{N_{\text{B}}}{k} \right\} \cdot \beta' \\ &= O \left(N_{\text{AP}}^2 \log N_{\text{AP}} \frac{2^k (\log N_{\text{CH}})^k}{k!} \right) \end{aligned} \quad (51)$$

for $3 \leq k \leq N_{\text{B}}$, while it is

$$\begin{aligned} G'_{k\text{-CR}} &= \binom{N_{\text{AP}}}{2} \binom{2N_{\text{B}}}{k} \cdot \beta' \\ &= O \left(N_{\text{AP}}^2 \log N_{\text{AP}} \frac{2^k (\log N_{\text{CH}})^k}{k!} \right) \end{aligned} \quad (52)$$

TABLE III
NUMBER OF QUANTUM GATES REQUIRED BY \mathbf{A}_{y_i} .

Gate	Conventional QUBO	Proposed HUBO
H	$O(N_{\text{AP}}^2)$	$O(N_{\text{AP}} \log N_{\text{AP}})$
R	$O(\log N_{\text{AP}})$	$O(\log N_{\text{AP}})$
1-CR	$O(N_{\text{AP}}^2 \log N_{\text{AP}})$	$O(N_{\text{AP}} (\log N_{\text{AP}})^2)$
2-CR	$O(N_{\text{AP}}^3 \log N_{\text{AP}})$	$O(N_{\text{AP}}^2 (\log N_{\text{AP}})^3)$
k -CR	0	$O(N_{\text{AP}}^2 (\log N_{\text{AP}})^{k+1}/k!)$
IQFT	1	1

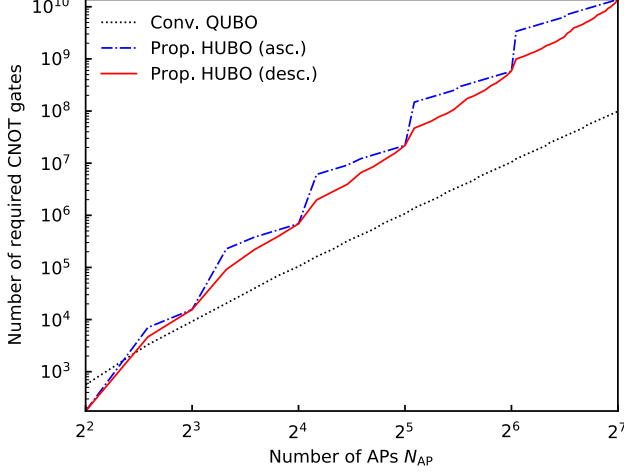


Fig. 6. Actual numbers of required CNOT gates.

for $N_B < k \leq 2N_B$.

From the results of the above analysis, the number of quantum gates required by the state preparation operator \mathbf{A}_{y_i} is summarized in Table III, where the number of channels is set to $N_{\text{CH}} = \lfloor N_{\text{AP}}/2 \rfloor$ for simplicity. Compared with the conventional formulation, the proposed formulation reduces the number of H gates, while it increases the total number of 1-CR, 2-CR, \dots , $(2N_B)$ -CR gates. The increase in the number of required gates is a major drawback of the proposed formulation.

To overcome this drawback, in Section IV, we proposed the descending binary encoding, which assigns a binary number to the channel index in descending order. In Fig. 6, we plot the effects of ascending and descending encodings, where the number of APs was increased from $N_{\text{AP}} = 2^2$ to 2^7 and the number of channels was $N_{\text{CH}} = \lfloor N_{\text{AP}}/2 \rfloor$. In actual quantum computers, the quantum circuit is decomposed into elementary gates [34]. After decomposition, the number of controlled NOT (CNOT) or T gates has been used to evaluate the complexity of quantum circuit [18, 23], termed as gate complexity. A 1-CR gate can be decomposed into elementary gates including two CNOT gates [34]. Using Maslov's approach [35] and relative-phase Toffoli gates, a decomposed n -CR gate has $6(n-1)$ CNOT gates. Then, we counted the total number of CNOT gates for both encodings.⁵ As shown in Fig. 6, the number of CNOT gates was reduced by

⁵Note that this decomposition requires ancilla qubits of $\deg(E(x)) - 1$ for QUBO and $\deg(E'(x)) - 1$ for HUBO, where $\deg(\cdot)$ is the degree of the objective function. This increase in ancilla qubits is negligible with respect to the number of required qubits $n + m$.

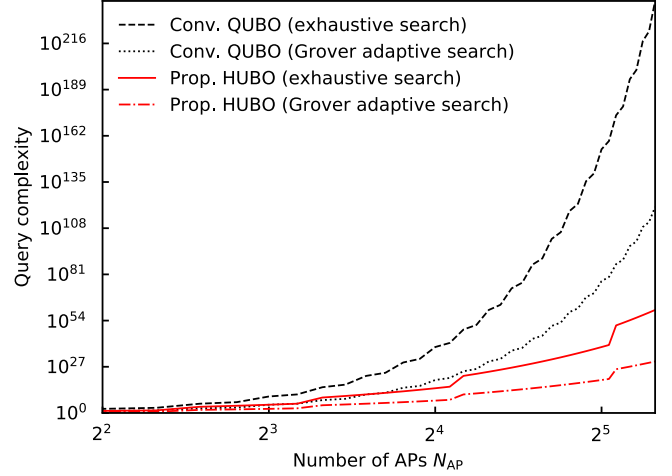


Fig. 7. Expected query complexity in the quantum domain.

the proposed descending encoding. Specifically, the difference between ascending and descending encodings was particularly large when $\log_2 N_{\text{AP}} \neq \lceil \log_2 N_{\text{AP}} \rceil$. We observed the same trend in our comparison of the number of T gates. Note that a particular gate decomposition method does not influence the relative advantages of different formulations. As the problem size increases, the gate complexity also increases correspondingly, which can lead to a fatal issue when using an actual quantum computer with gates that have finite fidelity.

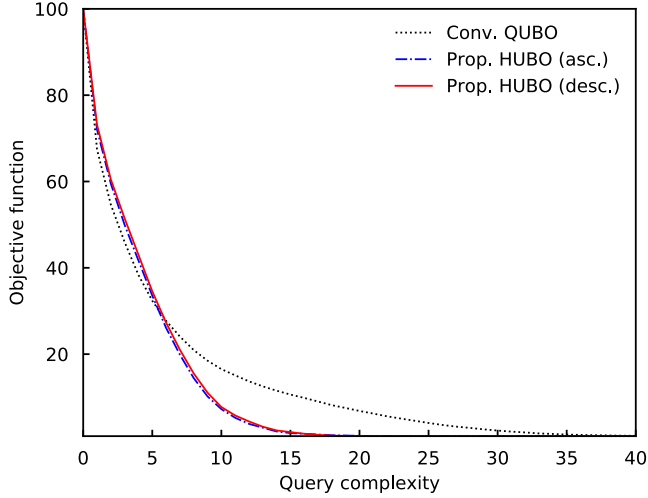
D. Query Complexity

Finally, we investigate the query complexities of GAS that are required by solving the conventional QUBO and the proposed HUBO formulations. As clarified in Section V-A, the conventional QUBO formulation requires $n = N_{\text{AP}} N_{\text{CH}}$ binary variables, while the proposed HUBO formulation requires $n' = N_{\text{AP}} \lceil \log_2 N_{\text{CH}} \rceil$ binary variables. Since GAS provides a quadratic speedup, the two query complexities are $\sqrt{2^n} = 2^{N_{\text{AP}} N_{\text{CH}}/2}$ and

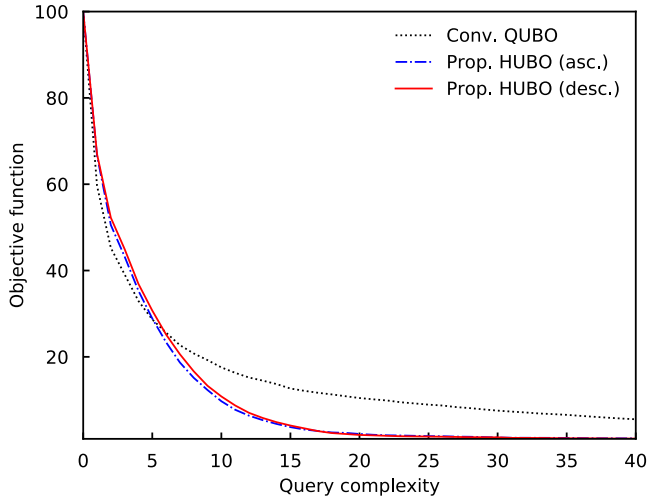
$$(N_{\text{CH}})^{\frac{N_{\text{AP}}}{2}} \leq \sqrt{2^{n'}} < (\sqrt{2} N_{\text{CH}})^{\frac{N_{\text{AP}}}{2}}, \quad (53)$$

respectively. Obviously, the reduction rate is maximized if $N_{\text{AP}} = N_{\text{CH}}$, and it becomes smaller as N_{CH} decreases. In Fig. 7, we show expected query complexities of both formulations, where the number of channels was $N_{\text{CH}} = \lfloor N_{\text{AP}}/2 \rfloor$. As a reference, the query complexity for the exhaustive search is also shown, which is equivalent to the average number of objective function evaluations. As shown in Fig. 7, the classic exhaustive search exhibited impractical complexities for both conventional and proposed formulations, and is infeasible on classical computers. By contrast, it can be expected that the proposed HUBO formulation using GAS significantly reduces the query complexity, and the reduction rate improves as the problem size increases.

In Fig. 8, we show the query complexities for the conventional and proposed formulations, which are given in Appendices A and B, respectively. Here, we set $N_{\text{AP}} = 4$ and $N_{\text{CH}} = 3$, evaluated the query complexity in the classical



(a) Query complexity in the classical domain.



(b) Query complexity in the quantum domain.

Fig. 8. Query complexities required by ideal GAS.

and quantum domains, and normalized the objective function values from 0 to 100. Our intention is to investigate how each formulation affects the query complexity, and due to the time-consuming nature of quantum simulations, we considered here an ideal GAS using the integer approximation [13] where the number of qubits to encode an objective function value, m , is sufficiently large. In all cases, the proposed HUBO formulation reached the optimal solution with reduced query complexity compared with the conventional QUBO formulation, which is the main advantage of the proposed formulation. This gap is expected to become large as the problem size increases, as given in Fig. 7. Additionally, as expected, both ascending and descending encodings exhibited the same query complexities. Each objective function includes real-valued coefficients. That is, when m is limited to a practical value, a degradation in query complexity is inferred from the conventional study [19] dealing with the real-valued GAS. However, this negative effect applies equally to the conventional and proposed formulations, and it does not affect their relative comparisons.

VI. CONCLUSIONS

In this paper, we formulated the NP-hard wireless CAP as a HUBO problem. To solve CAP, the conventional QUBO formulation uses the one-hot encoding of channel indices, while the proposed HUBO uses the ascending or descending binary encoding of the indices. The proposed formulation was analyzed in terms of the number of binary variables, the number of qubits, the number of gates, and the query complexity. When using GAS, we found that the proposed HUBO significantly reduced the number of qubits and the query complexity compared with the conventional QUBO formulation. This advantage was achieved at the cost of increased number of gates; however, the proposed descending binary encoding also succeeded in reducing the number of gates.

ACKNOWLEDGEMENT

The authors would like to thank Prof. Naoki Yamamoto, Keio University, Japan for providing valuable comments.

APPENDIX A

EXAMPLE OF QUBO FORMULATION

We describe the QUBO formulation for the case of $N_{AP} = 4$ and $N_{CH} = 3$, which was used in Fig. 8. We assume that the physical distances d_{iu} between the i th AP and u th UT for $1 \leq i \leq N_{AP}$ and $1 \leq u \leq 2N_{AP}$ in Fig. 2 are

$$\begin{aligned}
 & \begin{bmatrix} d_{11} & d_{12} & d_{13} & d_{14} & d_{15} & d_{16} & d_{17} & d_{18} \\ d_{21} & d_{22} & d_{23} & d_{24} & d_{25} & d_{26} & d_{27} & d_{28} \\ d_{31} & d_{32} & d_{33} & d_{34} & d_{35} & d_{36} & d_{37} & d_{38} \\ d_{41} & d_{42} & d_{43} & d_{44} & d_{45} & d_{46} & d_{47} & d_{48} \end{bmatrix} \\
 &= \begin{bmatrix} 1 & 1 & 2 & 4 & 3 & 5 & 5 & 8 \\ 5 & 4 & 1 & 1 & 5 & 4 & 2 & 4 \\ 6 & 5 & 2 & 5 & 1 & 1 & 4 & 6 \\ 10 & 8 & 5 & 2 & 5 & 3 & 1 & 1 \end{bmatrix}. \quad (54)
 \end{aligned}$$

Then, the scalar constant C_{ik} (18) for $1 \leq i < k \leq N_{AP}$ in Fig. 2 is calculated as

$$\begin{aligned}
 C_{12} &= -\log_2 \left(1 + \frac{1^{-1} + 1^{-1}}{2^{-1} + 4^{-1}} \right) - \log_2 \left(1 + \frac{1^{-1} + 1^{-1}}{5^{-1} + 4^{-1}} \right) = -4.319 \\
 C_{13} &= -\log_2 \left(1 + \frac{1^{-1} + 1^{-1}}{3^{-1} + 5^{-1}} \right) - \log_2 \left(1 + \frac{1^{-1} + 1^{-1}}{6^{-1} + 5^{-1}} \right) = -4.938 \\
 C_{14} &= -\log_2 \left(1 + \frac{1^{-1} + 1^{-1}}{5^{-1} + 8^{-1}} \right) - \log_2 \left(1 + \frac{1^{-1} + 1^{-1}}{10^{-1} + 8^{-1}} \right) = -6.145 \\
 C_{23} &= -\log_2 \left(1 + \frac{1^{-1} + 1^{-1}}{5^{-1} + 4^{-1}} \right) - \log_2 \left(1 + \frac{1^{-1} + 1^{-1}}{2^{-1} + 5^{-1}} \right) = -4.392 \\
 C_{24} &= -\log_2 \left(1 + \frac{1^{-1} + 1^{-1}}{2^{-1} + 4^{-1}} \right) - \log_2 \left(1 + \frac{1^{-1} + 1^{-1}}{5^{-1} + 2^{-1}} \right) = -3.822 \\
 C_{34} &= -\log_2 \left(1 + \frac{1^{-1} + 1^{-1}}{4^{-1} + 6^{-1}} \right) - \log_2 \left(1 + \frac{1^{-1} + 1^{-1}}{5^{-1} + 3^{-1}} \right) = -4.784 \quad (55)
 \end{aligned}$$

where we have the attenuation coefficient $\alpha = 1$ for simplicity. Now, we have $C_{\min} = -6.145$. The constants $D_{ik} = C_{ik} - C_{\min} + \epsilon$ (17) with $\epsilon = 0.01$ are calculated as $D_{12} = 1.835$, $D_{13} = 1.216$, $D_{14} = 0.010$, $D_{23} =$

1.762, $D_{24} = 2.333$, and $D_{34} = 1.371$. In this case, from (20), the conventional objective function is

$$\begin{aligned}
E(x) = & +1.835(x_{11}x_{21} + x_{12}x_{22} + x_{13}x_{23}) \\
& +1.216(x_{11}x_{31} + x_{12}x_{32} + x_{13}x_{33}) \\
& +0.010(x_{11}x_{41} + x_{12}x_{42} + x_{13}x_{43}) \\
& +1.762(x_{21}x_{31} + x_{22}x_{32} + x_{23}x_{33}) \\
& +2.333(x_{21}x_{41} + x_{22}x_{42} + x_{23}x_{43}) \\
& +1.371(x_{31}x_{41} + x_{32}x_{42} + x_{33}x_{43}) \\
& +(x_{11} + x_{12} + x_{13} - 1)^2 + (x_{21} + x_{22} + x_{23} - 1)^2 \\
& +(x_{31} + x_{32} + x_{33} - 1)^2 + (x_{41} + x_{42} + x_{43} - 1)^2.
\end{aligned} \tag{56}$$

The optimal solution is a set of binary vectors

$$\begin{aligned}
[x_{11} \ x_{12} \ x_{13}] &= [0 \ 1 \ 0] \rightarrow 2, \\
[x_{21} \ x_{22} \ x_{23}] &= [1 \ 0 \ 0] \rightarrow 1, \\
[x_{31} \ x_{32} \ x_{33}] &= [0 \ 0 \ 1] \rightarrow 3, \text{ and} \\
[x_{41} \ x_{42} \ x_{43}] &= [0 \ 1 \ 0] \rightarrow 2,
\end{aligned} \tag{57}$$

which are one-hot vectors. Solution (57) indicates that the first, second, third, and fourth APs use the second, first, third, and second channels, respectively.

APPENDIX B EXAMPLE OF HUBO FORMULATIONS

We describe the HUBO formulations for the case of $N_{\text{AP}} = 4$ and $N_{\text{CH}} = 3$ used in Fig. 8. Specifically, the proposed objective function using ascending encoding is given in (58), while that using descending encoding is given in (59). As given, the number of terms is reduced, i.e., from 67 to 55. The optimal solution for ascending encoding (58) is a set of binary vectors

$$\begin{aligned}
[x_{11} \ x_{12}] &= [0 \ 1] \rightarrow 2, \\
[x_{21} \ x_{22}] &= [0 \ 0] \rightarrow 1, \\
[x_{31} \ x_{32}] &= [1 \ 0] \rightarrow 3, \text{ and} \\
[x_{41} \ x_{42}] &= [0 \ 1] \rightarrow 2,
\end{aligned} \tag{60}$$

while the optimal solution for descending encoding (59) is a set of binary vectors

$$\begin{aligned}
[x_{11} \ x_{12}] &= [1 \ 0] \rightarrow 3, \\
[x_{21} \ x_{22}] &= [1 \ 1] \rightarrow 1, \\
[x_{31} \ x_{32}] &= [0 \ 1] \rightarrow 3, \text{ and} \\
[x_{41} \ x_{42}] &= [1 \ 0] \rightarrow 2.
\end{aligned} \tag{61}$$

Both solutions indicate the same situation as that given in (57).

REFERENCES

- [1] ITU, "IMT traffic estimates for the years 2020 to 2030," *Report ITU-R*, vol. 2370-0, Jul. 2015.
- [2] W. Hale, "Frequency assignment: Theory and applications," *Proceedings of the IEEE*, vol. 68, no. 12, pp. 1497–1514, Dec. 1980.
- [3] S. Ramanathan, "A unified framework and algorithm for channel assignment in wireless networks," *Wireless Networks*, vol. 5, no. 2, pp. 81–94, Mar. 1999.
- [4] J. Kwok and K. Pudenz, "Graph coloring with quantum annealing," *arXiv:2012.04470 [quant-ph]*, Dec. 2020.
- [5] C. Wang, H. Chen, and E. Jonckheere, "Quantum versus simulated annealing in wireless interference network optimization," *Scientific Reports*, vol. 6, no. 1, p. 25797, May 2016.
- [6] K. Saito, A. Ikami, and C. Ono, "Evaluating dynamic spectrum allocation using quantum annealing," *IEICE Communications Express*, vol. 10, no. 9, pp. 726–732, Jun. 2021.
- [7] R. Hamerly, T. Inagaki, P. L. McMahon, D. Venturelli, A. Marandi, T. Onodera, E. Ng, C. Langrock, K. Inaba, T. Honjo, K. Enbutsu, T. Umeki, R. Kasahara, S. Utsunomiya, S. Kako, K. Kawarabayashi, R. L. Byer, M. M. Fejer, H. Mabuchi, D. Englund, E. Rieffel, H. Takesue, and Y. Yamamoto, "Experimental investigation of performance differences between coherent Ising machines and a quantum annealer," *Science Advances*, vol. 5, no. 5, May 2019.
- [8] K. Inaba, T. Inagaki, K. Igarashi, S. Utsunomiya, T. Honjo, T. Ikuta, K. Enbutsu, T. Umeki, R. Kasahara, K. Inoue, Y. Yamamoto, and H. Takesue, "Potts model solver based on hybrid physical and digital architecture," *Communications Physics*, vol. 5, May 2022.
- [9] H. Ito, Y. Jiang, H. Yasuda, H. Takesue, K. Aihara, and M. Hasegawa, "High-speed optimization method for resource allocation in wireless communication systems by coherent Ising machine," in *International Conference on Artificial Intelligence in Information and Communication*, Fukuoka, Japan, Feb. 19–21, 2020.
- [10] M. Hasegawa, H. Ito, H. Takesue, and K. Aihara, "Optimization by neural networks in the coherent Ising machine and its application to wireless communication systems," *IEICE Transactions on Communications*, vol. E104.B, no. 3, pp. 210–216, Mar. 2021.
- [11] K. Kurasawa, K. Hashimoto, A. Li, K. Sato, K. Inaba, H. Takesue, K. Aihara, and M. Hasegawa, "A high-speed channel assignment algorithm for dense IEEE 802.11 systems via coherent Ising machine," *IEEE Wireless Communications Letters*, vol. 10, no. 8, pp. 1682–1686, Aug. 2021.
- [12] P. Botsinis, D. Alanis, Z. Babar, H. V. Nguyen, D. Chandra, S. X. Ng, and L. Hanzo, "Quantum search algorithms for wireless communications," *IEEE Communications Surveys & Tutorials*, vol. 21, no. 2, pp. 1209–1242, Secondquarter 2019.
- [13] A. Gilliam, S. Woerner, and C. Gondiulea, "Grover adaptive search for constrained polynomial binary optimization," *Quantum*, vol. 5, p. 428, Apr. 2021.
- [14] A. Gilliam, M. Pistoia, and C. Gondiulea, "Optimizing quantum search using a generalized version of Grover's algorithm," *arXiv:2005.06468 [quant-ph]*, May 2020.
- [15] L. K. Grover, "A fast quantum mechanical algorithm for database search," in *ACM Symposium on Theory of Computing*, Philadelphia, Pennsylvania, USA, May 22–24, Jul. 1996.
- [16] M. Boyer, G. Brassard, P. Hoyer, and A. Tapp, "Tight bounds on quantum searching," *Fortschritte der Physik*, vol. 46, no. 4–5, pp. 493–505, Apr. 1998.
- [17] C. Durr and P. Hoyer, "A quantum algorithm for finding the minimum," *arXiv:quant-ph/9607014*, Jan. 1999.
- [18] H. Tezuka, K. Nakaji, T. Satoh, and N. Yamamoto, "Grover search revisited: Application to image pattern matching," *Physical Review A*, vol. 105, no. 3, p. 032440, Mar. 2022.
- [19] M. Norimoto, R. Mori, and N. Ishikawa, "Quantum algorithm for higher-order unconstrained binary optimization and MIMO maximum likelihood detection," *IEEE Transactions on Communications*, vol. 71, no. 4, pp. 1926–1939, Apr. 2023.
- [20] L. Giuffrida, D. Volpe, G. A. Cirillo, M. Zamboni, and G. Turvani, "Engineering Grover adaptive search: Exploring the degrees of freedom for efficient QUBO solving," *IEEE Journal on Emerging and Selected Topics in Circuits and Systems*, vol. 12, no. 3, pp. 614–623, Sep. 2022.
- [21] K. Yukiyoishi and N. Ishikawa, "Quantum search algorithm for binary constant weight codes," *arXiv:2211.04637 [quant-ph]*, Nov. 2022.
- [22] K. Fujii, "Noise threshold of quantum supremacy," *arXiv:1610.03632 [quant-ph]*, Oct. 2016.
- [23] C. Gidney and M. Ekerå, "How to factor 2048 bit RSA integers in 8 hours using 20 million noisy qubits," *Quantum*, vol. 5, p. 433, Apr. 2021.
- [24] N. P. D. Sawaya, T. Menke, T. H. Kyaw, S. Johri, A. Aspuru-Guzik, and G. G. Guerreschi, "Resource-efficient digital quantum simulation of d-level systems for photonic, vibrational, and spin-s Hamiltonians," *npj Quantum Information*, vol. 6, no. 1, pp. 1–13, Jun. 2020.
- [25] P. Larrañaga, C. Kuijpers, R. Murga, I. Inza, and S. Dizdarevic, "Genetic algorithms for the travelling salesman problem: A review of representations and operators," *Artificial Intelligence Review*, vol. 13, no. 2, pp. 129–170, Apr. 1999.
- [26] F. G. Fuchs, H. Ø. Kolden, N. H. Aase, and G. Sartor, "Efficient encoding of the weighted max k -cut on a quantum computer using

$$\begin{aligned}
E'_a(x) = & +1.835\{(1-x_{11})(1-x_{12})(1-x_{21})(1-x_{22}) + (1-x_{11})x_{12}(1-x_{21})x_{22} + x_{11}(1-x_{12})x_{21}(1-x_{22})\} \\
& +1.216\{(1-x_{11})(1-x_{12})(1-x_{31})(1-x_{32}) + (1-x_{11})x_{12}(1-x_{31})x_{32} + x_{11}(1-x_{12})x_{31}(1-x_{32})\} \\
& +0.010\{(1-x_{11})(1-x_{12})(1-x_{41})(1-x_{42}) + (1-x_{11})x_{12}(1-x_{41})x_{42} + x_{11}(1-x_{12})x_{41}(1-x_{42})\} \\
& +1.762\{(1-x_{21})(1-x_{22})(1-x_{31})(1-x_{32}) + (1-x_{21})x_{22}(1-x_{31})x_{32} + x_{21}(1-x_{22})x_{31}(1-x_{32})\} \\
& +2.333\{(1-x_{21})(1-x_{22})(1-x_{41})(1-x_{42}) + (1-x_{21})x_{22}(1-x_{41})x_{42} + x_{21}(1-x_{22})x_{41}(1-x_{42})\} \\
& +1.371\{(1-x_{31})(1-x_{32})(1-x_{41})(1-x_{42}) + (1-x_{31})x_{32}(1-x_{41})x_{42} + x_{31}(1-x_{32})x_{41}(1-x_{42})\} \\
& +x_{11}x_{12} + x_{21}x_{22} + x_{31}x_{32} + x_{41}x_{42}
\end{aligned} \tag{58}$$

$$\begin{aligned}
E'_d(x) = & +1.835\{x_{11}x_{12}x_{21}x_{22} + x_{11}(1-x_{12})x_{21}(1-x_{22}) + (1-x_{11})x_{12}(1-x_{21})x_{22}\} \\
& +1.216\{x_{11}x_{12}x_{31}x_{32} + x_{11}(1-x_{12})x_{31}(1-x_{32}) + (1-x_{11})x_{12}(1-x_{31})x_{32}\} \\
& +0.010\{x_{11}x_{12}x_{41}x_{42} + x_{11}(1-x_{12})x_{41}(1-x_{42}) + (1-x_{11})x_{12}(1-x_{41})x_{42}\} \\
& +1.762\{x_{21}x_{22}x_{31}x_{32} + x_{21}(1-x_{22})x_{31}(1-x_{32}) + (1-x_{21})x_{22}(1-x_{31})x_{32}\} \\
& +2.333\{x_{21}x_{22}x_{41}x_{42} + x_{21}(1-x_{22})x_{41}(1-x_{42}) + (1-x_{21})x_{22}(1-x_{41})x_{42}\} \\
& +1.371\{x_{31}x_{32}x_{41}x_{42} + x_{31}(1-x_{32})x_{41}(1-x_{42}) + (1-x_{31})x_{32}(1-x_{41})x_{42}\} \\
& -(1-x_{11})(1-x_{12}) + (1-x_{21})(1-x_{22}) + (1-x_{31})(1-x_{32}) + (1-x_{41})(1-x_{42})
\end{aligned} \tag{59}$$

QAOA,” *SN Computer Science*, vol. 2, no. 2, p. 89, Feb. 2021.

- [27] A. Glos, A. Krawiec, and Z. Zimborás, “Space-efficient binary optimization for variational quantum computing,” *npj Quantum Information*, vol. 8, no. 1, pp. 1–8, Apr. 2022.
- [28] Z. Tabi, K. H. El-Safty, Z. Kallus, P. Hága, T. Kozsik, A. Glos, and Z. Zimborás, “Quantum optimization for the graph coloring problem with space-efficient embedding,” in *IEEE International Conference on Quantum Computing and Engineering*, Denver, CO, USA, Oct. 12–16, 2020.
- [29] Z. Luo, W. Ma, A. M. So, Y. Ye, and S. Zhang, “Semidefinite relaxation of quadratic optimization problems,” *IEEE Signal Processing Magazine*, vol. 27, no. 3, pp. 20–34, May 2010.
- [30] I. G. Rosenberg, “Reduction of bivalent maximization to the quadratic case,” *Cahiers du Centre d’Etudes de Recherche Operationnelle*, vol. 17, pp. 71–74, Jan. 1975.
- [31] M. Anthony, E. Boros, Y. Crama, and A. Gruber, “Quadratic reformulations of nonlinear binary optimization problems,” *Mathematical Programming*, vol. 162, no. 1, pp. 115–144, Mar. 2017.
- [32] W. P. Baritompa, D. W. Bulger, and G. R. Wood, “Grover’s quantum algorithm applied to global optimization,” *SIAM Journal on Optimization*, vol. 15, no. 4, pp. 1170–1184, Jan. 2005.
- [33] D. E. Knuth, “Big Omicron and big Omega and big Theta,” *ACM SIGACT News*, vol. 8, no. 2, pp. 18–24, 1976.
- [34] M. A. Nielsen and I. L. Chuang, *Quantum Computation and Quantum Information*. Cambridge ; New York: Cambridge University Press, 2010.
- [35] D. Maslov, “Advantages of using relative-phase Toffoli gates with an application to multiple control Toffoli optimization,” *Physical Review A*, vol. 93, no. 2, p. 022311, Feb. 2016.

Naoki Ishikawa (Senior Member, IEEE) is an Associate Professor with the Faculty of Engineering, Yokohama National University, Kanagawa, Japan. He received the B.E., M.E., and Ph.D. degrees in electronic and information engineering from the Tokyo University of Agriculture and Technology, Tokyo, Japan, in 2014, 2015, and 2017, respectively. In 2015, he was an academic visitor with the School of Electronics and Computer Science, University of Southampton, UK. From 2016 to 2017, he was a research fellow of the Japan Society for the Promotion of Science. From 2017 to 2020, he was an assistant professor in the Graduate School of Information Sciences, Hiroshima City University, Japan. He was certified as an Exemplary Reviewer of IEEE TRANSACTIONS ON COMMUNICATIONS in 2017 and 2021. His research interests include massive MIMO, physical layer security, and quantum speedup for wireless communications.

Yuki Sano received the B.E. degree in engineering science from Iwate University, Iwate, Japan, in 2021, and the M.E. degree in engineering science from Yokohama National University, Kanagawa, Japan, in 2023. He is currently working at Nomura Research Institute based in Tokyo.

Masaya Norimoto (Graduate Student Member, IEEE) received the B.E. degree in engineering science from Yokohama National University, Kanagawa, Japan, in 2022. He is currently pursuing the M.E. degree with the Graduate School of Engineering Science, Yokohama National University, Kanagawa, Japan. His research interests include quantum algorithms and wireless communications.